Supporting Information for:

Bioinspired superhydrophobic polylactic acid aerogel with tree branch structure for the removal of viscous oil spills assisted by solar energy

Yihao Guan [a, b,d], Bingqian Bi [a, b], Di Qiao [a, b], Sijing Cao [a, b], Wenjun Zhang [a, b], Zhining Wang [c], Hongbo Zeng [d], Yiming Li [a, b, *]

[a] *Frontiers Science Center for Deep Ocean Multispheres and Earth System/Key Laboratory of Marine Chemistry Theory and Technology, Ministry of Education, Ocean University of China, 266100, Qingdao, P.R. China*

[b] *College of Chemistry & Chemical Engineering, Ocean University of China, Qingdao 266100, P.R. China*

[c] *Shandong Key Laboratory of Water Pollution Control and Resource Reuse, School of Environmental Science and Engineering, Shandong University, Qingdao 266237, P.R. China*

[d] *Department of Chemical and Materials Engineering, University of Alberta, Edmonton, Alberta T6G 1H9, Canada*

[*] Corresponding author.
E-mail address: liym@ouc.edu.cn (Y.M. Li)

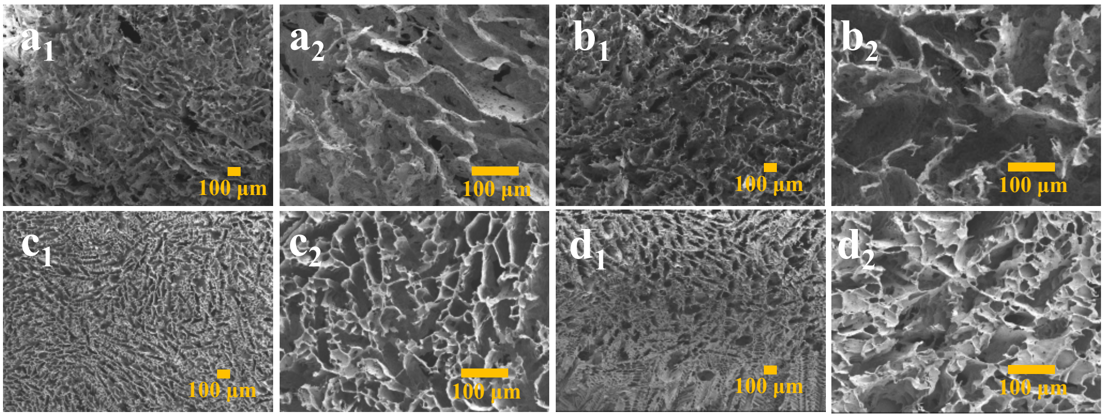

Fig. S1 SEM images of PLA aerogel prepared from different PLA concentrations (a) 10 %, (b) 20 %, (c) 30 %, and (d) 40 %.

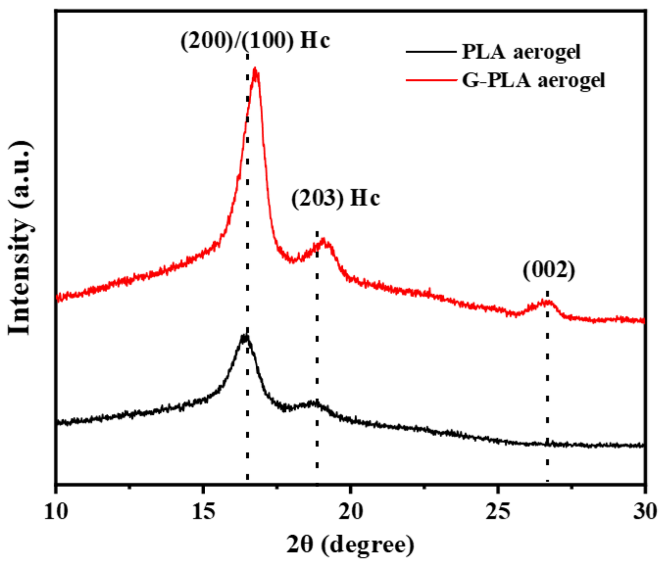

Fig. S2 XRD spectrum of PLA and G-PLA aerogel.

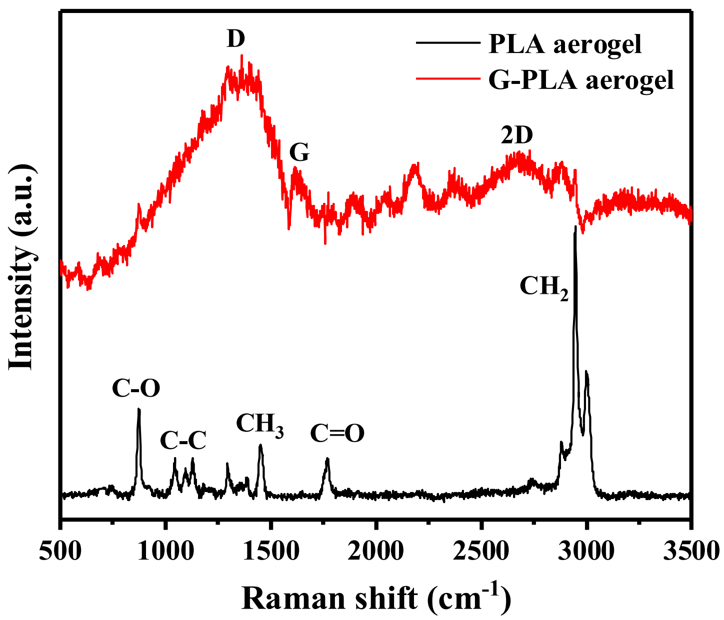

Fig. S3 Raman spectrum of PLA and G-PLA aerogel.

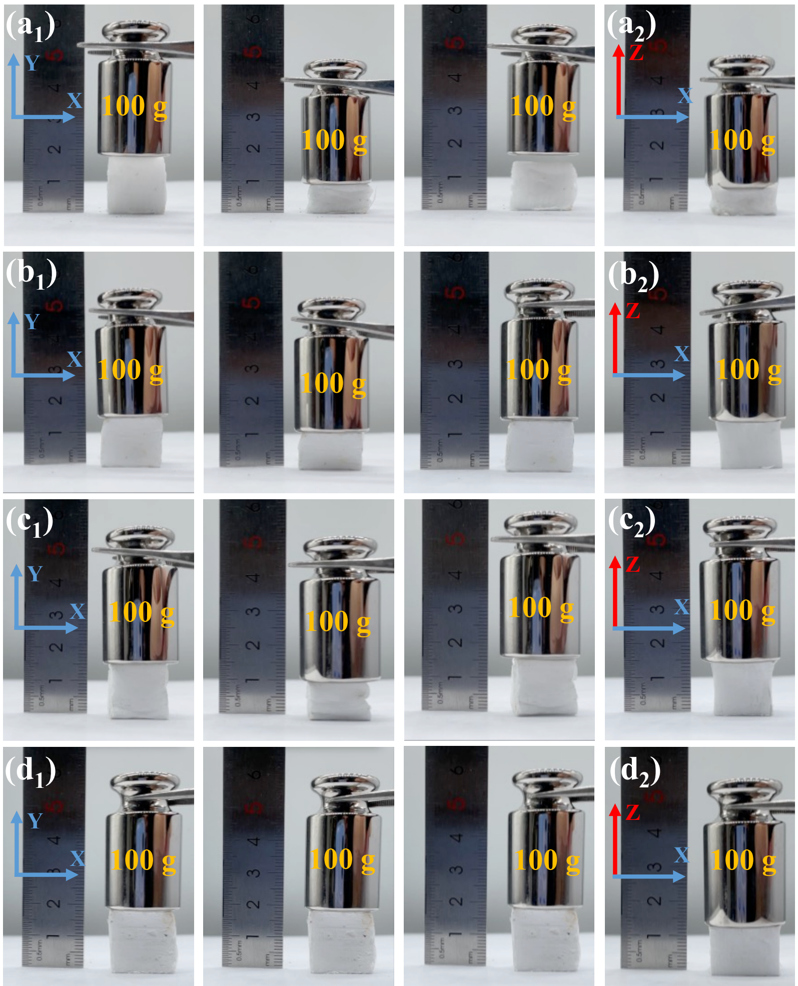

Fig. S4 Shape recovery of the (a) 10 % PLA, (b) 20 % PLA, (c) 30 %PLA, and (d) 40 % PLA aerogel after being compressed by a weight of 100 g.

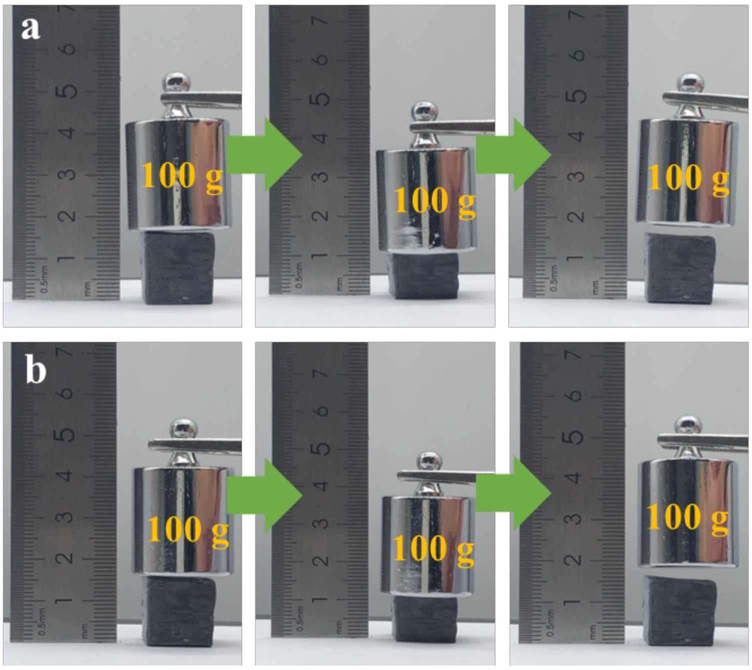

Fig. S5 Shape recovery of the G-PLA aerogel after being compressed by a weight of 100 g, and the graphene content are (a) 2 % and (b) 6 %, respectively.

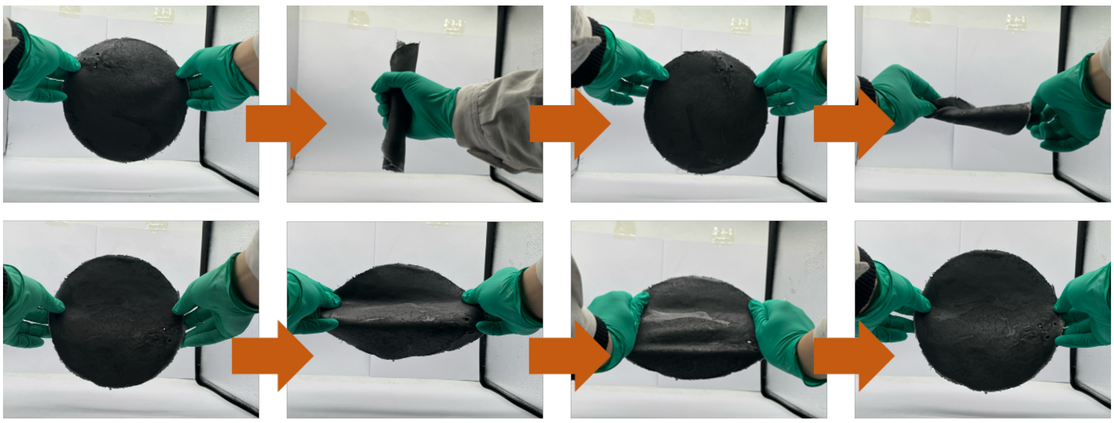

Fig. S6 G-PLA aerogel bending, twisting, and stretching test.

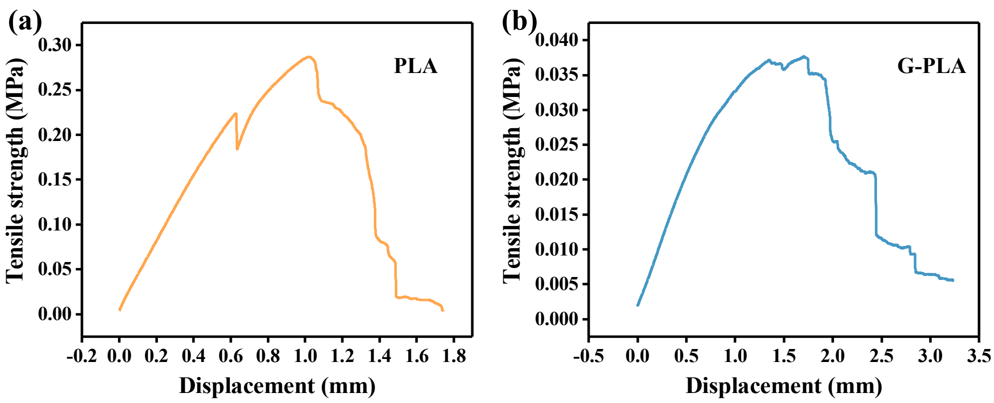

Fig. S7 Tensile properties of (a) PLA aerogel, and (b) G-PLA aerogel.

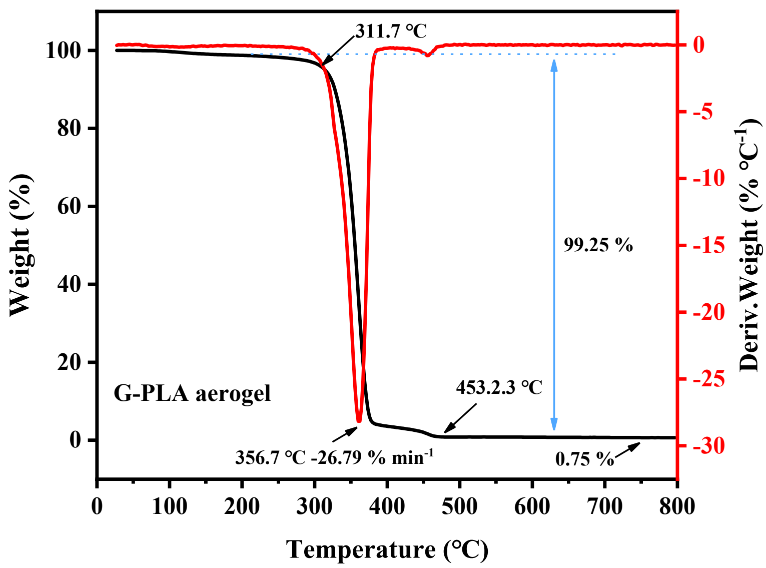

Fig. S8 TGA diagrams and DTG analysis of G-PLA aerogel.

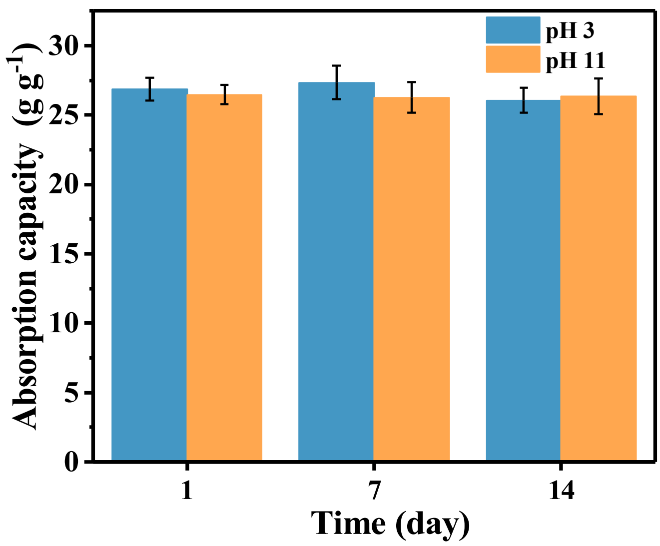

Fig. S9 The crude oil absorption of G-PLA aerogel immersing in pH 3, and pH 11 solutions after 7 and 14 days.

Fig. S10 Photographs of PLA (left) and G-PLA (right) aerogel in diesel/water mixture.

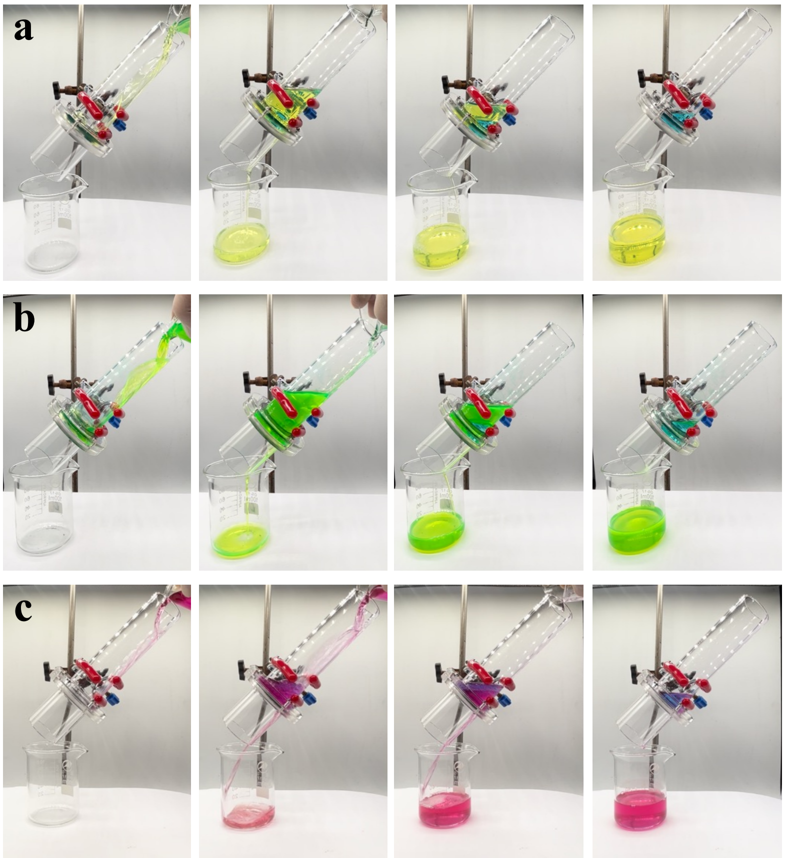

Fig. S11 Photographs of G-PLA aerogel for a mixture of water and diesel (a), kerosene (b), and CCl_4 (c), respectively.

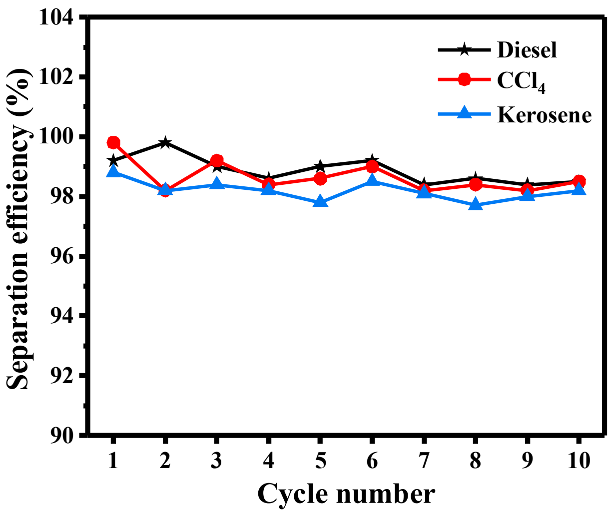

Fig. S12 Cycles separation efficiency of G-PLA aerogel for a mixture of water and diesel, kerosene, and CCl_4, respectively.

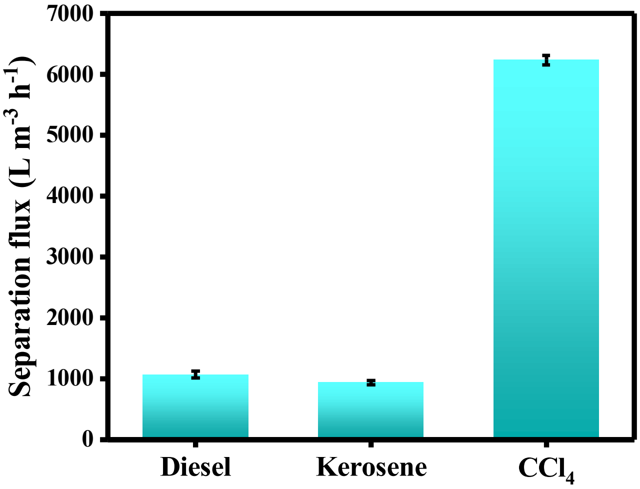

Fig. S13 Separation flux of G-PLA aerogel for a mixture of water and diesel, kerosene, and CCl_4, respectively.

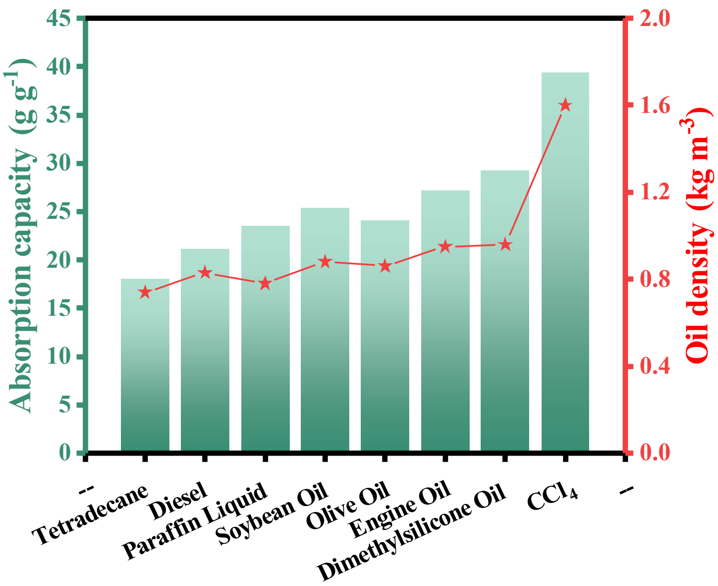

Fig. S14 Absorption capacity of the G-PLA aerogel for various oils or organic solvents.

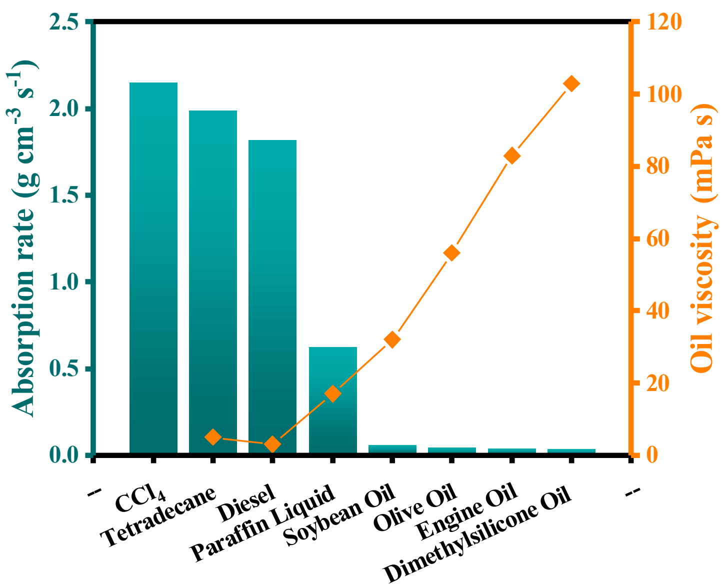

Fig. S15 Absorption rate of the G-PLA aerogel for various oils or organic solvents with different viscosities.

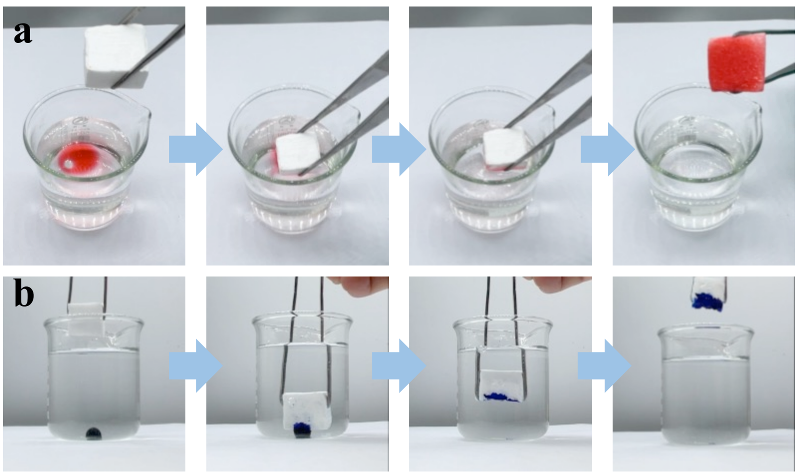

Fig. S16 Photographs showing (a) removal of diesel from the water surface and (b) trichloromethane underwater by the G-PLA aerogel.

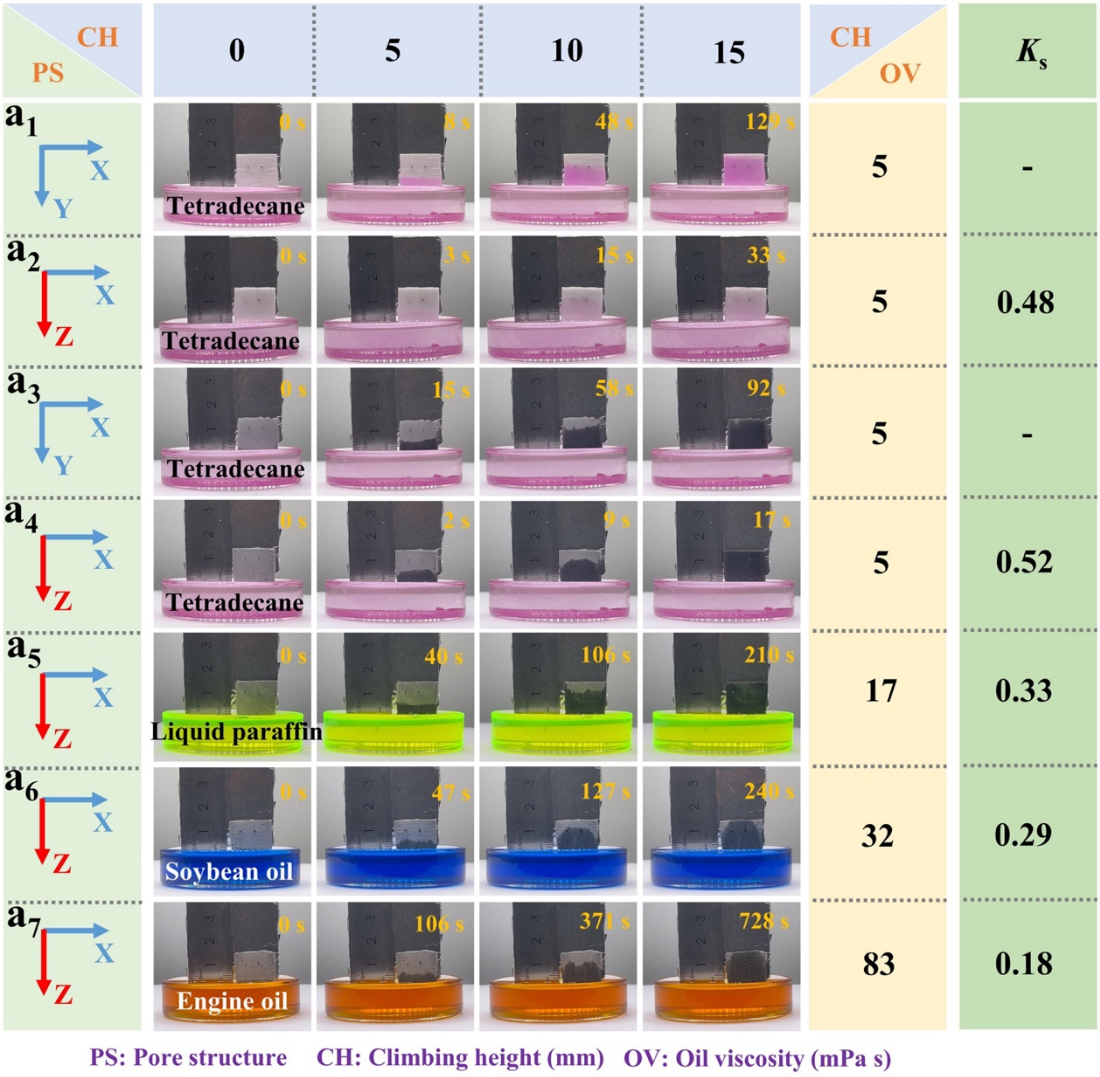

Fig. 17 Successive optical images showing distinct absorbing rate of oils with different viscosities inside the different porous structures: (a_1) random pores and (a_2) aligned channels of PLA aerogel, (a_3) random pores and (a_4- a_7) aligned channels of G-PLA aerogel.

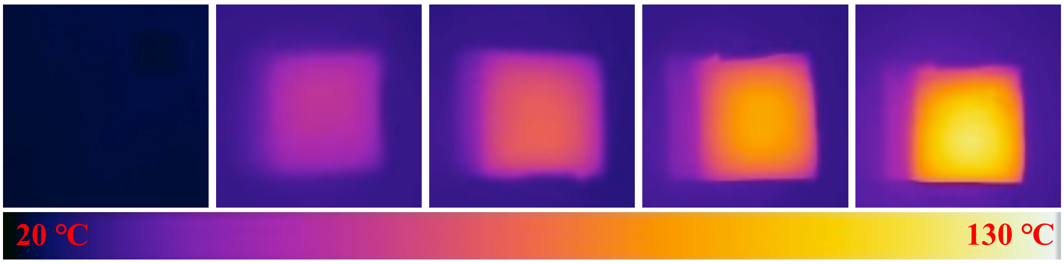

Fig. S18 IR images of G-PLA aerogel under simulated sunlight irradiation (kW m^{-2}) of 0, 0.5, 1.0, 1.5, and 2.0 from left to right.

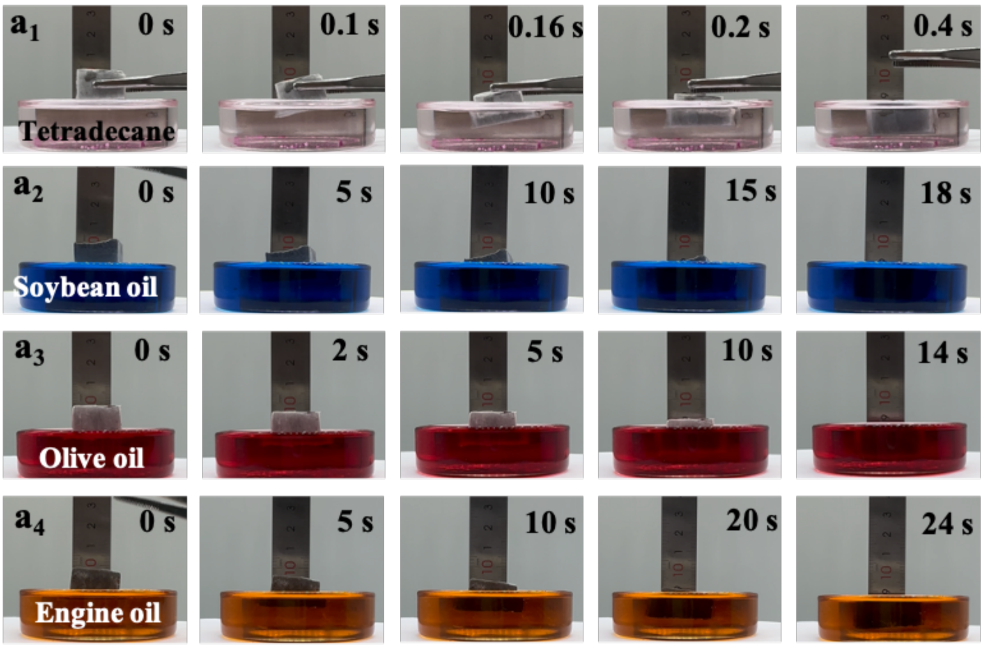

Fig. S19 Photographs showing the sinking behavior of G-PLA aerogel in different types of oils under no sunlight.

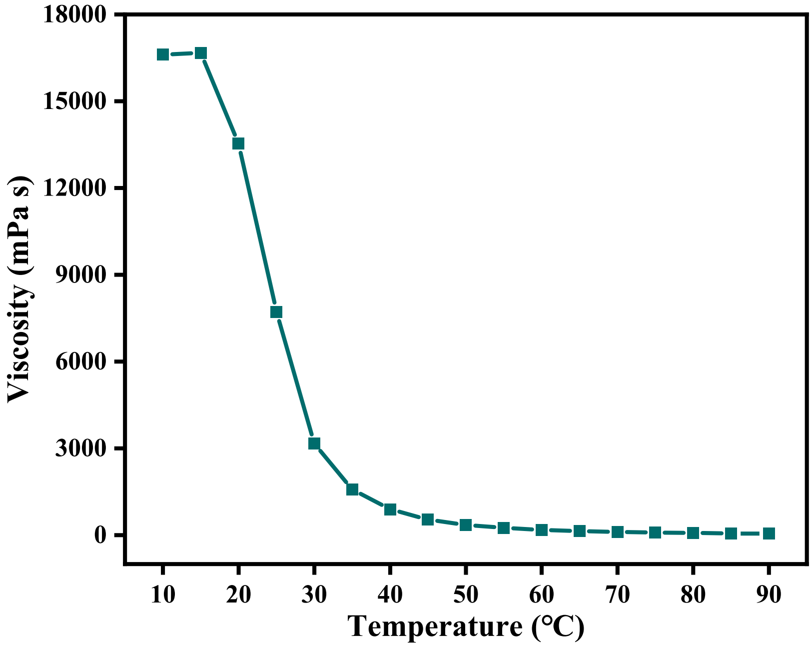

Fig. S20 The variance of crude oil viscosity with temperature.

Fig. S21 Photographs showing the sinking behavior of G-PLA aerogel in the absence of sunlight irradiation.

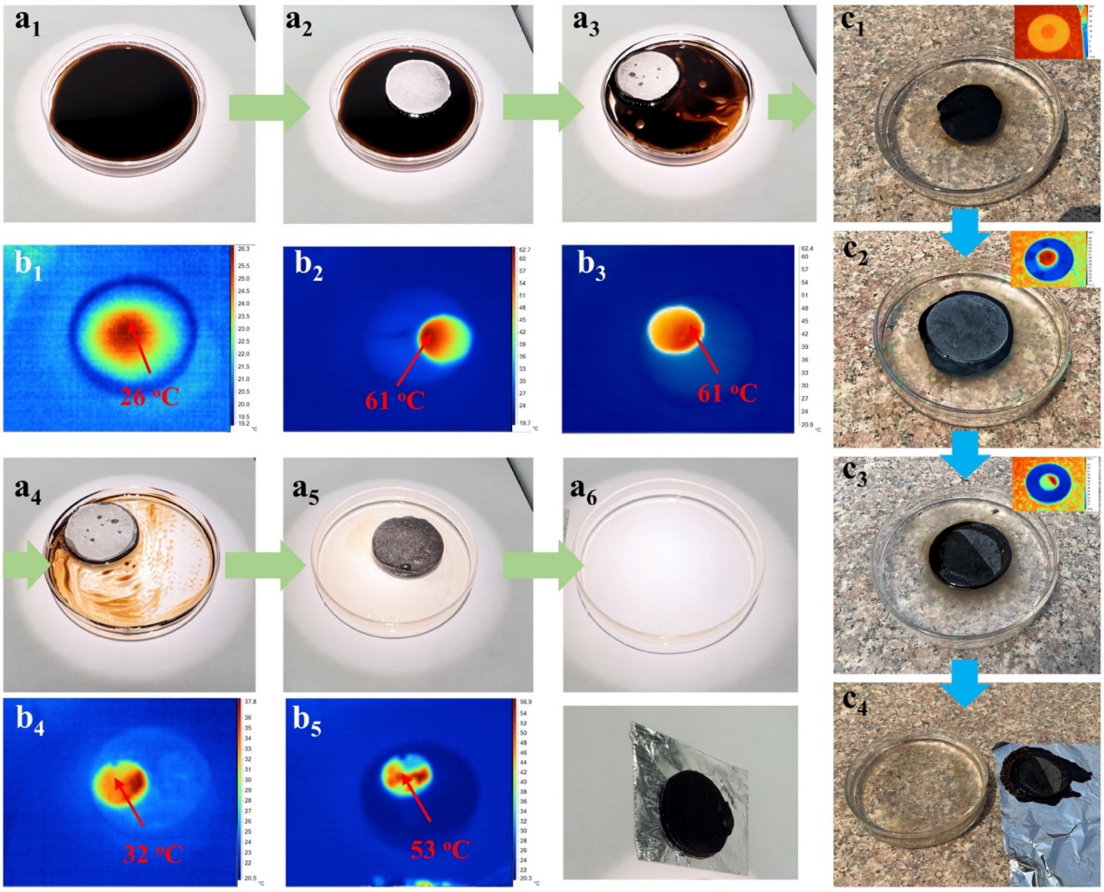

Fig. S22 The optical photos and corresponding infrared thermal imaging of G-PLA aerogel in absorbing crude oil on the sea surface at (a, b) laboratory (1 kW m^{-2} light intensity), and (c) outdoors (13:00).

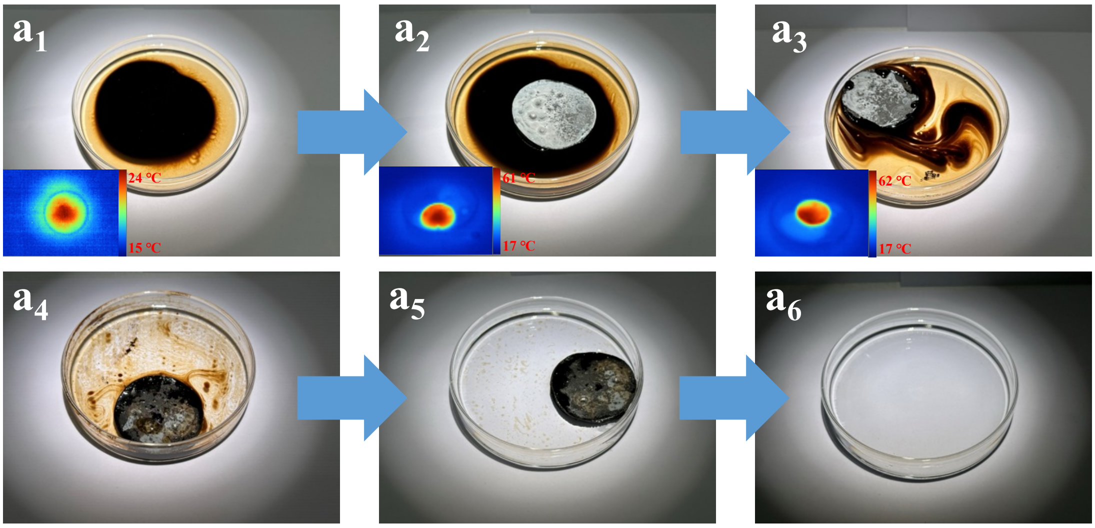

Fig. S23 The optical photos and corresponding infrared thermal imaging of G-PLA aerogel in absorbing crude oil on the sea surface, and the seawater collected in Qingdao Shilaoren Beach.

Table S1: Parameters of different types of oils

	Density (kg m^{-3})	Viscosity (mPa s)	Surface tension (mN m^{-1})
Tetradecane	0.76	5	26.5
Liquid paraffin	0.88	17	25.6
Soybean oil	0.92	32	35.2
Engine oil	0.95	83	34.6